

**Technical Report 1603**

April 1993

**Residual Strain Measurement  
on the Production-Grade  
Class IV Flextensional  
Transducer Shell**

J. D. Maltby

## **SUMMARY**

### **OBJECTIVE**

Empirically determine the residual strain of the production-grade Class IV flextensional transducer shell produced by Brunswick Defense.

### **RESULTS**

Residual stresses deduced from the strain measurements indicate that they are both additive to and in opposition to the localized stress states experienced by the shell in-service.

### **CONCLUSIONS**

The test data revealed that the inside fibers of the shell were under residual tension and the outside fibers were under residual compression. The residual stresses tend to be a small percentage of critical in-service stresses.

## CONTENTS

SUMMARY .....	i
BACKGROUND .....	1
SHELL CHARACTERISTICS .....	1
PROCEDURES .....	1
RESULTS .....	10
DISCUSSION .....	10
CONCLUSIONS .....	16
REFERENCES .....	17
<b>FIGURES</b>	
1a. Locations of all gage placements. ....	2
1b. Closeup of gage placements at ring's end. ....	3
1c. Closeup of gage placements at ring's midbay flat. ....	3
2. Dimensions of gages. ....	4
3. Instrumented ring ready for sectioning. ....	7
4a. Closeup of gages placed at ring's end. ....	8
4b. Closeup of gages placed at ring's midbay flat. ....	8
5. Cutting the ring. ....	9
6. Picture of first saw cut. ....	11
7. Locations and successive order of saw cuts. ....	11
8. Ring pieced together after completing all cuts. ....	12
9a. Longitudinal strains recorded after cutting. ....	12
9b. Normal strains recorded after cutting. ....	13
9c. Shear strains recorded after cutting. ....	13
<b>TABLES</b>	
1. Strain gage layout. ....	5
2. Final strain values after completing saw cuts. ....	14
3. Engineering constants of Brunswick shells. ....	14
4. Residual stresses. ....	15
5. Critical stresses experienced under hydrostatic pressure (reference 7). ....	16
6. Residual stresses compared to critical stresses listed in table 5. ....	16

## **BACKGROUND**

The oval-shaped shells used in one particular Class IV flextensional transducer are filament wound from fiberglass/epoxy by Brunswick Defense, Lincoln, NE. Lockheed Sanders Surveillance Systems Division, Manchester, NH, prime contractor for the transducer, purchases these shells from Brunswick.

Early in the development of the transducer shell—when Du Pont was fabricating the shells—process-induced residual stresses were a concern in structural failures (reference 1). Although Brunswick has not suffered similar problems, the residual stress information is still important to obtain a thorough understanding of the structural behavior of the shells. It is possible that residual stresses can still be a critical component to the long term stability of the shells, and residual stress information is important to any failure prediction methodologies.

Analytical prediction of residual stresses in a composite structure is not trivial. Processing variables determine these stresses. Brunswick uses proprietary techniques to manufacture their shells.

In the past, structural tests on transducer shells were conducted with the aid of rosette strain gages to assess the strain field through the shell thickness (reference 2). A similar approach was undertaken in this work.

## **SHELL CHARACTERISTICS**

Residual strains were measured on a standard transducer shell segment (8.67 inches wide) that was manufactured by Brunswick in March 1992. This was during the time that Brunswick was under contract to build a production lot of transducer shells for Sanders. The purchased shell was specified to be built in the same manner and configuration as the production shells.

The glass filaments used in the shells supplied by Brunswick are E-glass. The fiber orientation is unidirectional, aligned perpendicular to the windowing axis (i.e., “hoop” wound). The shells are wound on an aluminum mandrel.

Further information on the characteristics of these shells is found in reference 3.

## **PROCEDURES**

### **SUMMARY**

Residual strains were measured at discrete locations with electric resistance strain gages. The shell was sawed completely through its thickness at each gage location on each side of the gages to relieve the strains that were geometrically locked in. The measured difference in strain between the uncut state (i.e., the “zero strain” state) and the cut state provided the desired

residual strain information. Essentially, *macrostrain* states were measured; the resolution being no finer than the size of the strain gage grid.

Residual stresses are one component contributing to the total stress state of shells. The residual stress state varies as a function of temperature. In this report, we only consider the residual strains of the shell at room temperature.

## PROCEDURE DETAILS

A 2-inch-wide ring was removed from the purchased shell for testing. The ring was cut with a diamond impregnated circular saw blade mounted horizontally on a vertical knee-mill. This left a rather rough end-surface.

Strain gages were mounted on the inside surface and on the much smoother end-surface that Brunswick cut by using their standard production methods. The end-surface of the shell was further smoothed by hand with a sanding block at all of the gage locations prior to gage placement.

Gages were selectively placed at critical locations on the shell (figures 1a, b, and c). Table 1 lists all of the locations and the type of gage used at those locations. Gage type CEA-13-125UW-350 is a general purpose single gage; gage type CEA-06-062UR-350 is a small 45° rectangular single-plane rosette. The dimensions of the two gage types are depicted in figure 2.

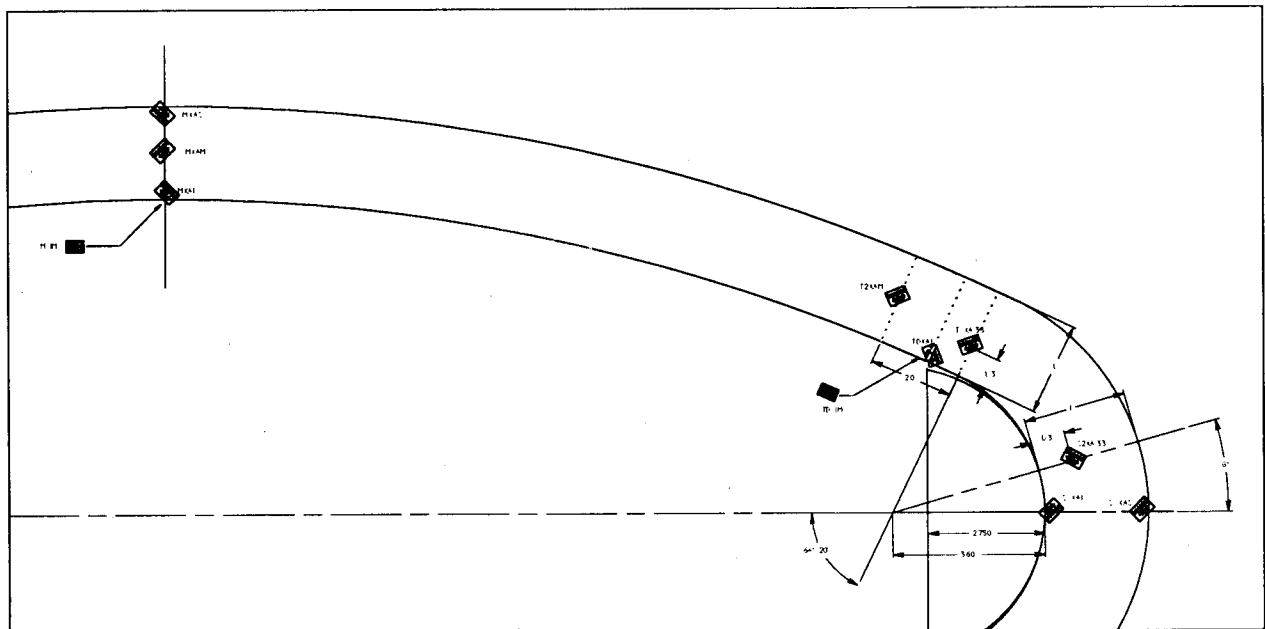


Figure 1a. Locations of all gage placements.

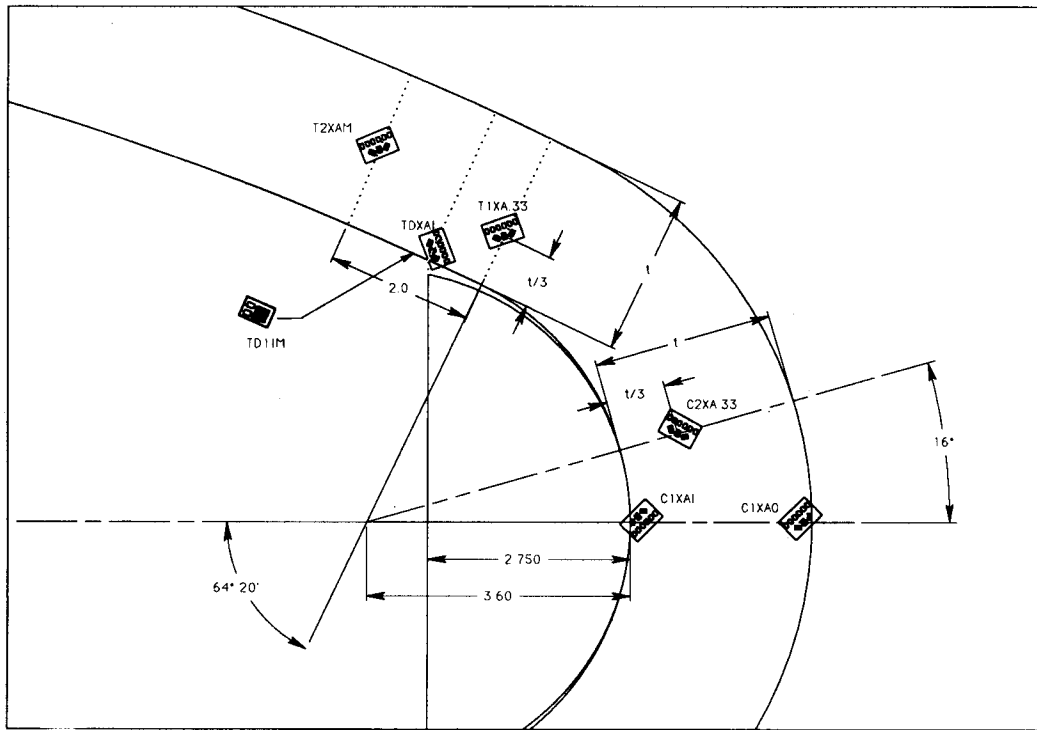


Figure 1b. Closeup of gage placements at ring's end.

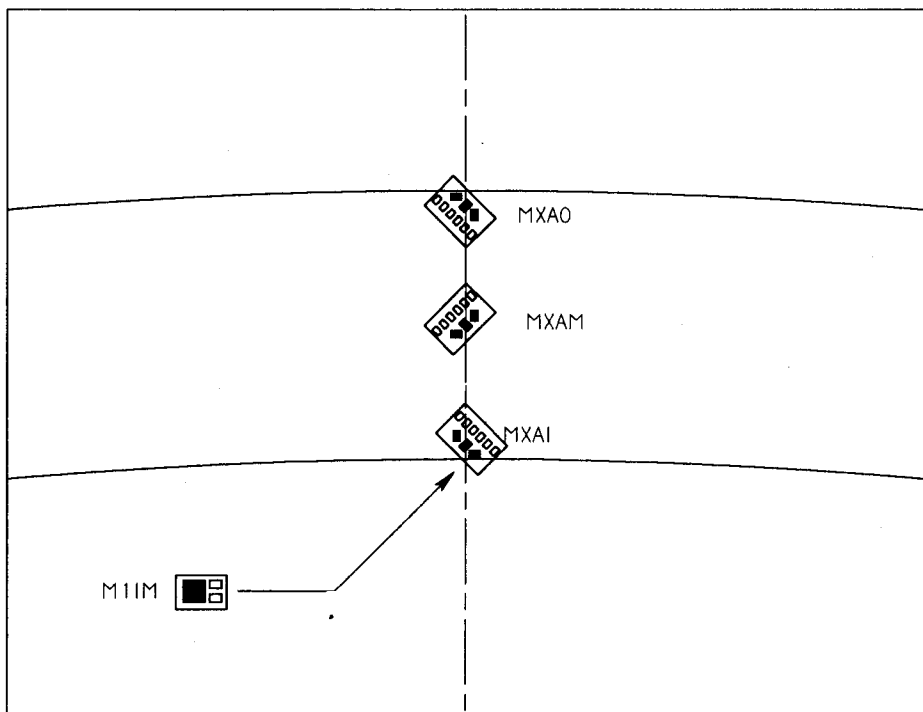
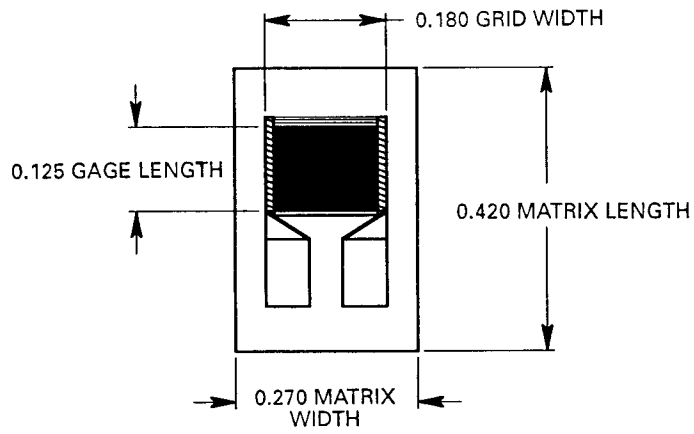
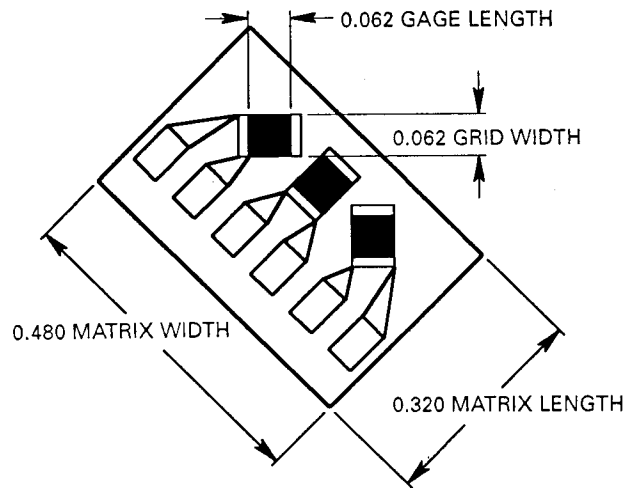


Figure 1c. Closeup of gage placements at ring's midbay flat.



AXIAL GAGE



RECTANGULAR ROSETTE

Figure 2. Dimensions of gages.

Table 1. Strain gage layout.

Location	Orientation	Gage Type	Gage Factor
MXAI	N	CEA-062UR-350	$2.10 \pm 1.0\%$
	S+	"	"
	L	"	"
MXAM	N	-Gage was lost-	—
	S-	CEA-06-062UR-350	$2.10 \pm 1.0\%$
	L	"	"
MXAO	N	"	"
	S+	"	"
	L	"	"
T2XAM	N	"	"
	S-	"	"
	L	"	"
TDXAI	N	"	"
	S+	"	"
	L	"	"
T1XA.33	N	"	"
	S-	"	"
	L	"	"
C2XA.33	N	"	"
	S-	"	"
	L	"	"
C1XAO	N	"	"
	S+	"	"
	L	"	"
M1IM	L	CEA-13-125UW-350	$2.13 \pm 1.0\%$
TD1IM	L	"	"

## LOCATION SYNTAX

The gage syntax was similar to that used for the work reported in reference 3. Gages placed on the cross-sectional surface of the shell have an X in their location name. The first one or two characters before the X indicates the circumferential location of the gage around the shell's quarter section as follows:

*M* Midbay location—situated halfway down the shell's major axis;

*T1* Transition location—where the end radius (3.583 inches) and the radius through the flat (approximately 43.2 inches) meet;

*TD* Transition location—defined as the intersection of the front normal surface of the transducer's D-insert and the inside surface of the shell;

*T2* Transition location—further down the shell quadrant, a chord distance of 2 inches from location *T1* measured along the inside surface;

*C2* Curve location—16° off of the shell's major axis; and

*C1* Curve location—directly on the shell's major axis.

The *A* in the location name indicates that all the gages are placed on the same cross-sectional side of the ring. The last letter of the name indicates whether the gage was placed near the shell's inside surface (*I*), in the middle of the shell thickness (*M*), or near its outside surface (*O*). Gages with the fractional number 0.33 at the end of their name (rather than a letter) were placed at a distance equal to 1/3 of the thickness from the shell's inside surface. These fractional locations were particularly selected because of the high-shear stresses that occur at these locations under the transducer's operational conditions (reference 4).

Each of the rectangular rosettes was oriented such that one of its gages was running parallel (denoted in table 1 with an *L* for longitudinal) to the fibers; one was perpendicular (denoted as *N* for normal) to the fibers; and one was oriented 45° with respect to the fiber direction (denoted as *S* for shear). The suffix after the *S* in table 1 clarifies further the orientation of the 45° shear gage. It is either positive 45° (denoted with a "+") or negative 45° (denoted with a "-") with respect to the fiber direction, as seen in figure 1. Figure 3 is a picture of the instrumented ring.

The two gages placed on the inside surface of the ring (locations *M1IM* and *TD1IM*) were oriented longitudinally in the middle of the ring's width.

Closeups of the gage placements are found in figures 4a and 4b.

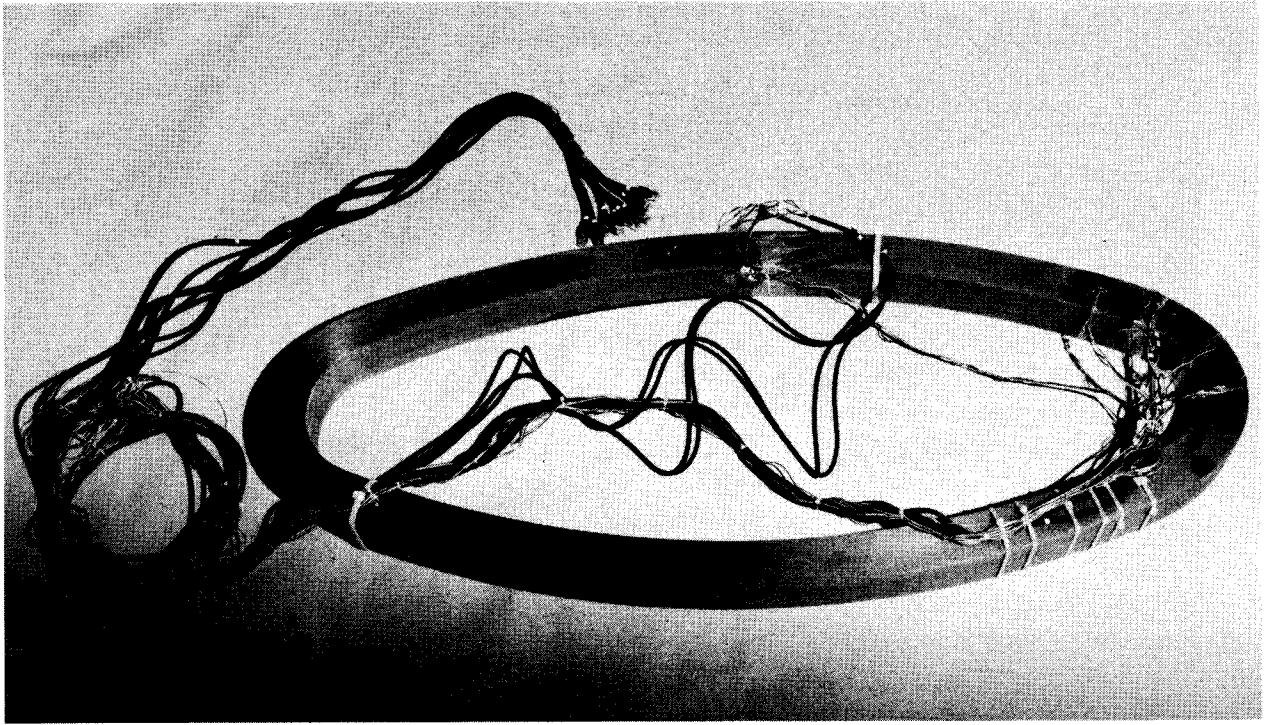


Figure 3. Instrumented ring ready for sectioning.

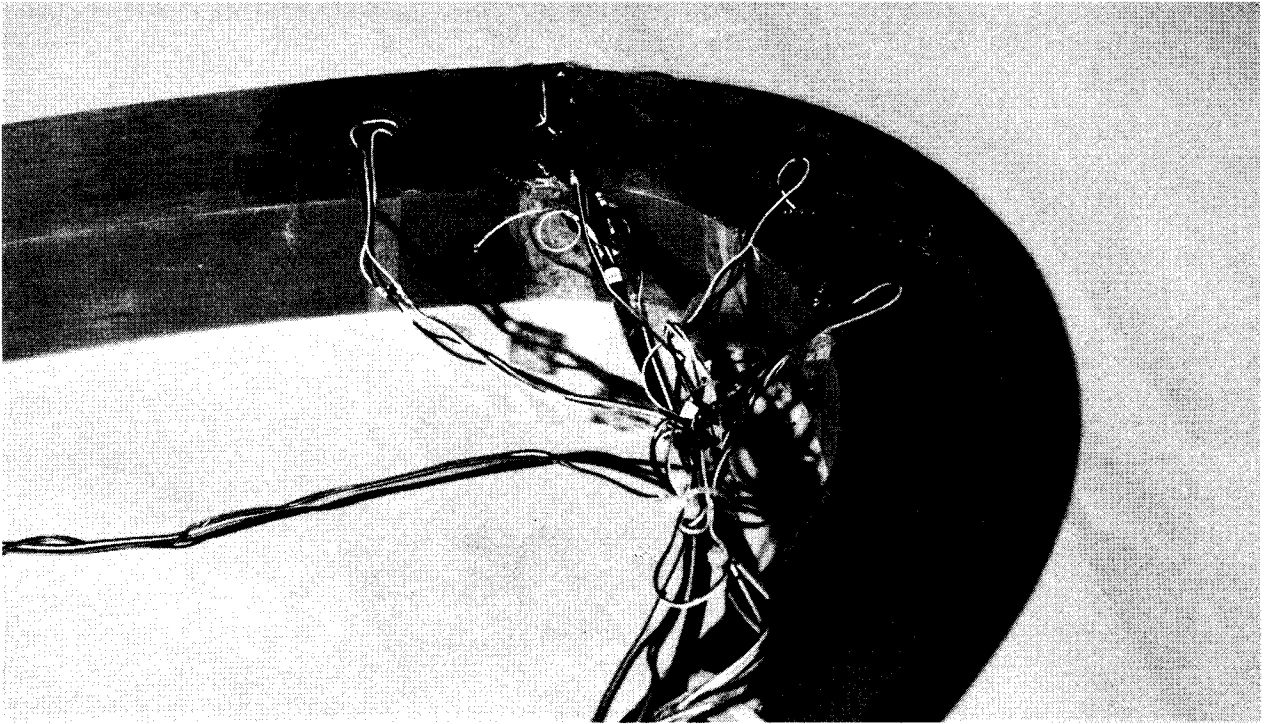


Figure 4a. Closeup of gages placed at ring's end.

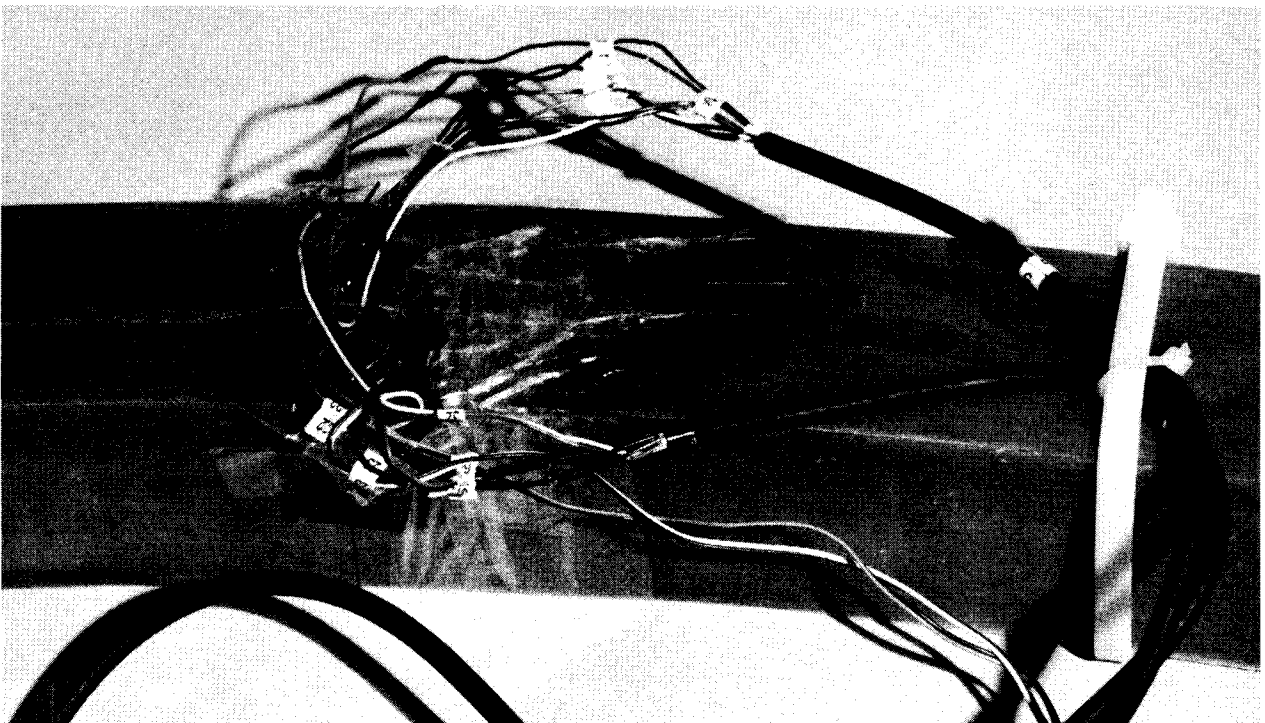


Figure 4b. Closeup of gages placed at ring's midbay flat.

## RING CUTTING

A bandsaw was used to cut the ring by using a carbide-impregnated blade (figure 5). Prior to cutting the ring, the gages were “zeroed” and the first data point was recorded. Data points were recorded after each cut.

During the first cut, a tremendous clamping pressure was placed on the blade as residual stress was relieved in the shell. The clamping pressure was so great that it was not possible to cut completely through the ring until a makeshift jack, placed along the major axis of the ring, was employed to push the sectioned sides apart. A screwdriver was also used to pry apart the sections at the cut.

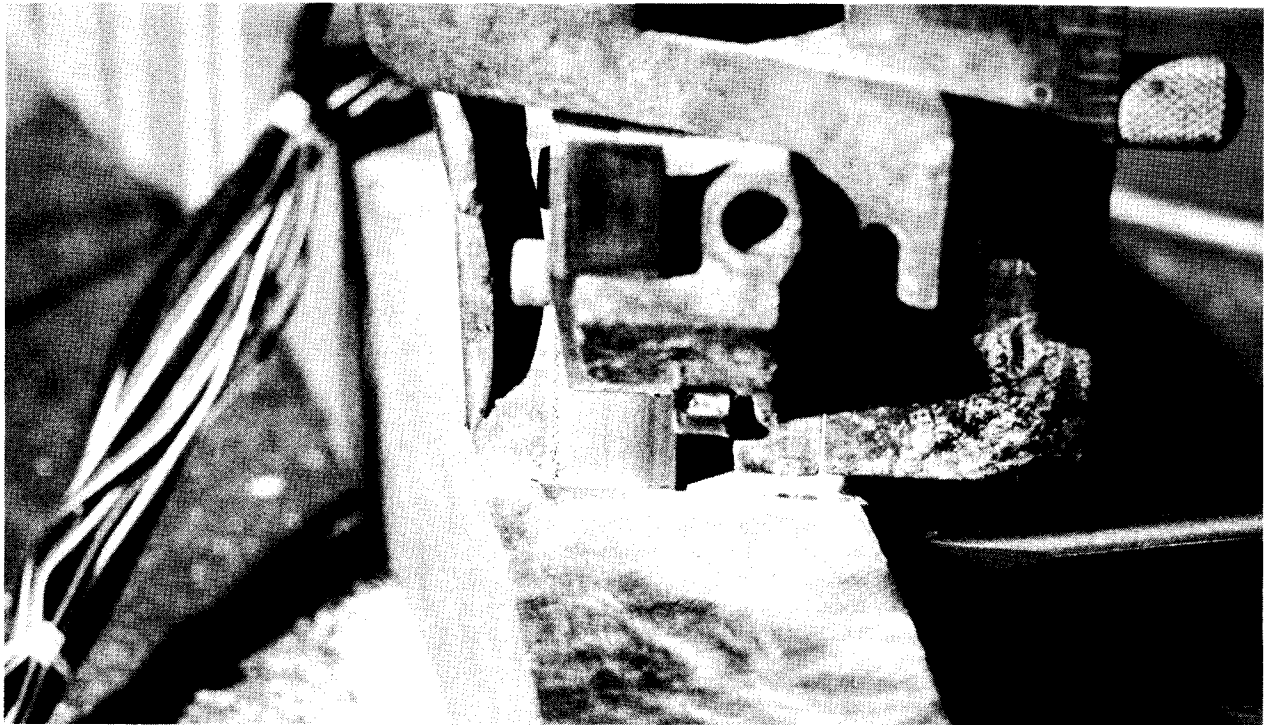


Figure 5. Cutting the ring.

Figure 6 shows the first saw cut after the blade was removed. The face sections were tightly clamped together and one face was displaced from the other due to relief of residual stress in the ring.

Cuts were made as close as practical to the gages without damaging the strain gage wires. Nine cuts were made on the ring; the successive order in which they were made and their locations are depicted in figure 7. Figure 8 shows the ring sections pieced together after all the cuts were completed.

## RESULTS

The final strain values after all cuts were made are tabulated in table 2. These strains values are depicted on the shell at their respective locations in figures 9a–9c.

## DISCUSSION

Residual strains that were geometrically locked into the shell are of the opposite sign to those measured after cutting (table 2), which is why the table lists them as recorded strains rather than residual strains. For example, at the midbay flat inside surface (i.e., gage location M1IM), a residual tensile strain of 950 microstrain existed prior to cutting. Conversely, those locations where strain of positive sign was recorded were under residual compression.

Stress values can be computed from the strains by using Hooke's law and the proper engineering constants. Table 3 lists engineering constants used in finite element modeling (reference 5) of the Brunswick shells and indicates the coordinate orientations that will be assumed.

The generalized Hooke's law is greatly simplified because the material is transversely isotropic in the 1–3 plane. The concise constitutive relationships to determine stresses in the 1–2 plane are listed as follows:

$$\begin{Bmatrix} \sigma_1 \\ \sigma_2 \\ \sigma_5 \end{Bmatrix} = \begin{bmatrix} C_{11} & C_{12} & C_{12} & 0 \\ C_{21} & C_{22} & C_{23} & 0 \\ 0 & 0 & 0 & C_{55} \end{bmatrix} \begin{Bmatrix} e_1 \\ e_2 \\ e_3 \\ e_5 \end{Bmatrix}$$

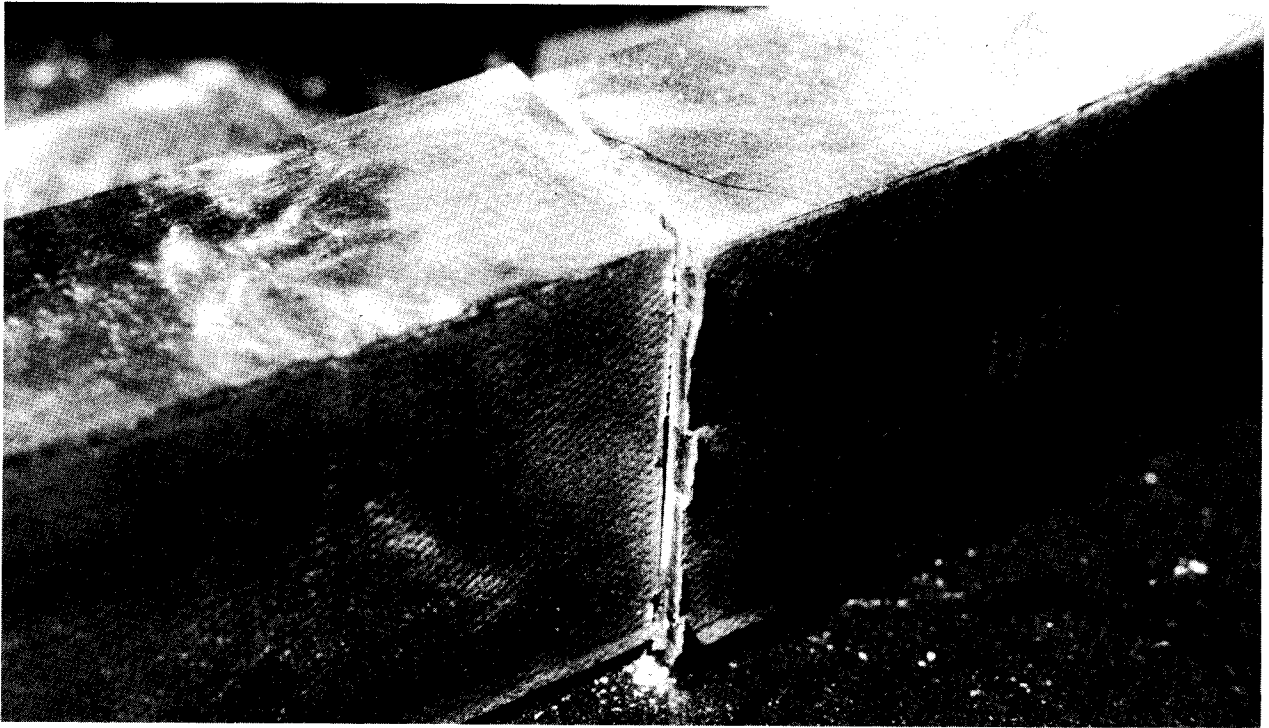


Figure 6. Picture of first saw cut.

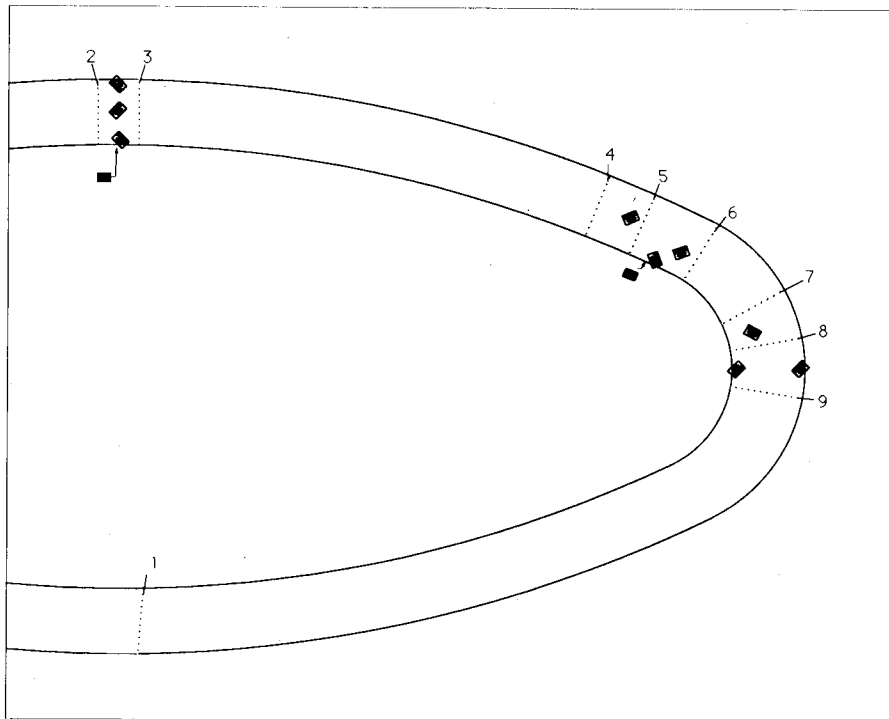


Figure 7. Locations and successive order of saw cuts.

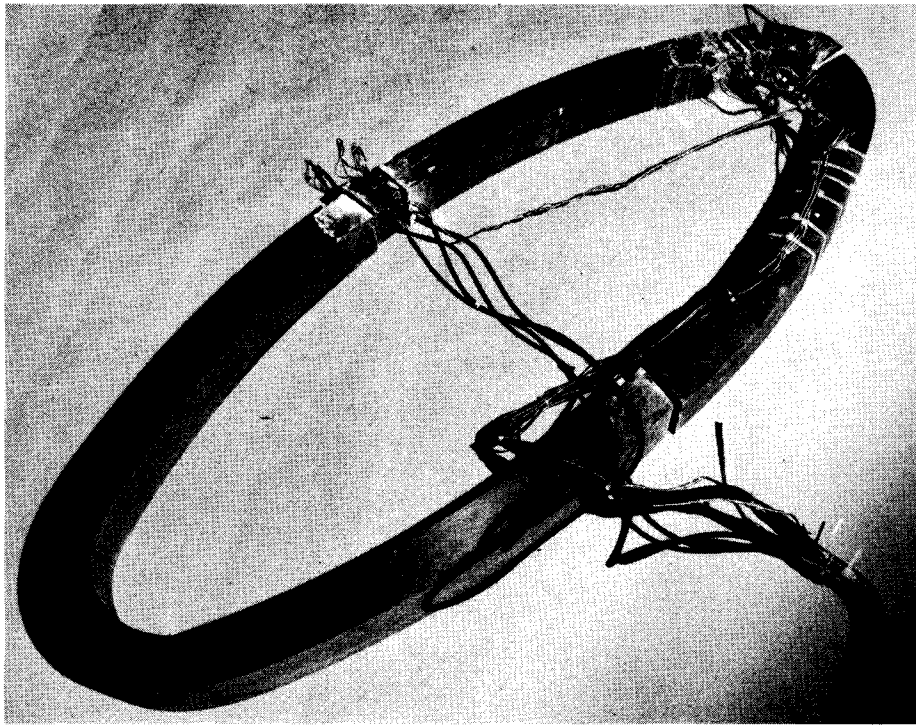


Figure 8. Ring pieced together after completing all cuts.

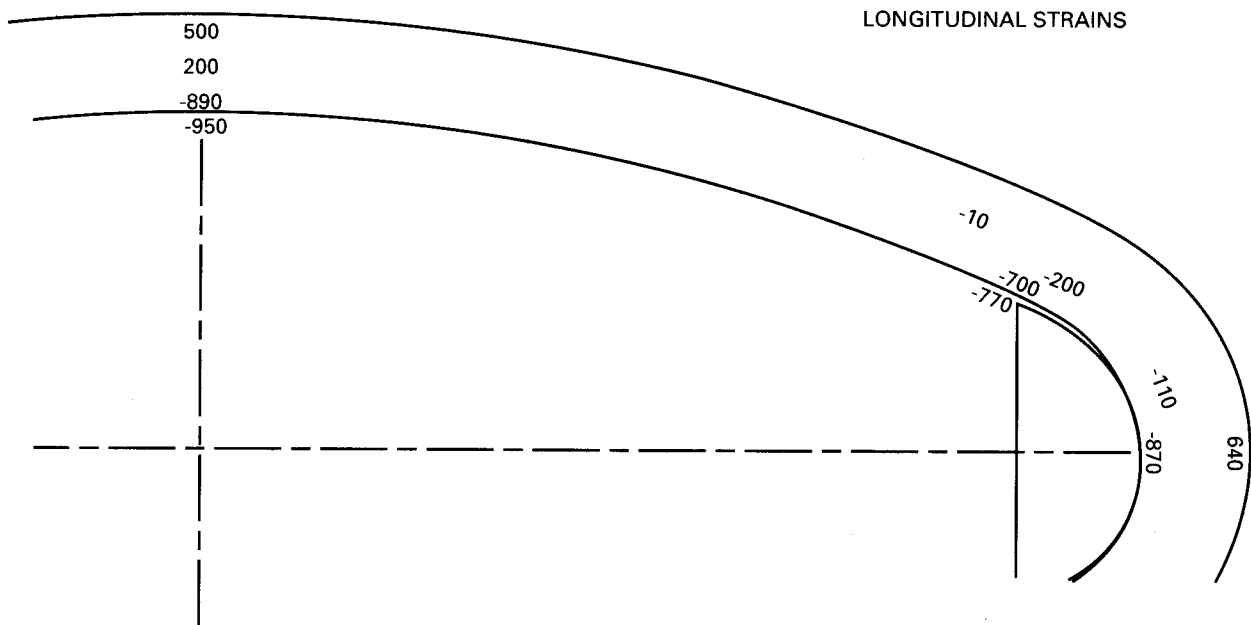


Figure 9a. Longitudinal strains recorded after cutting.

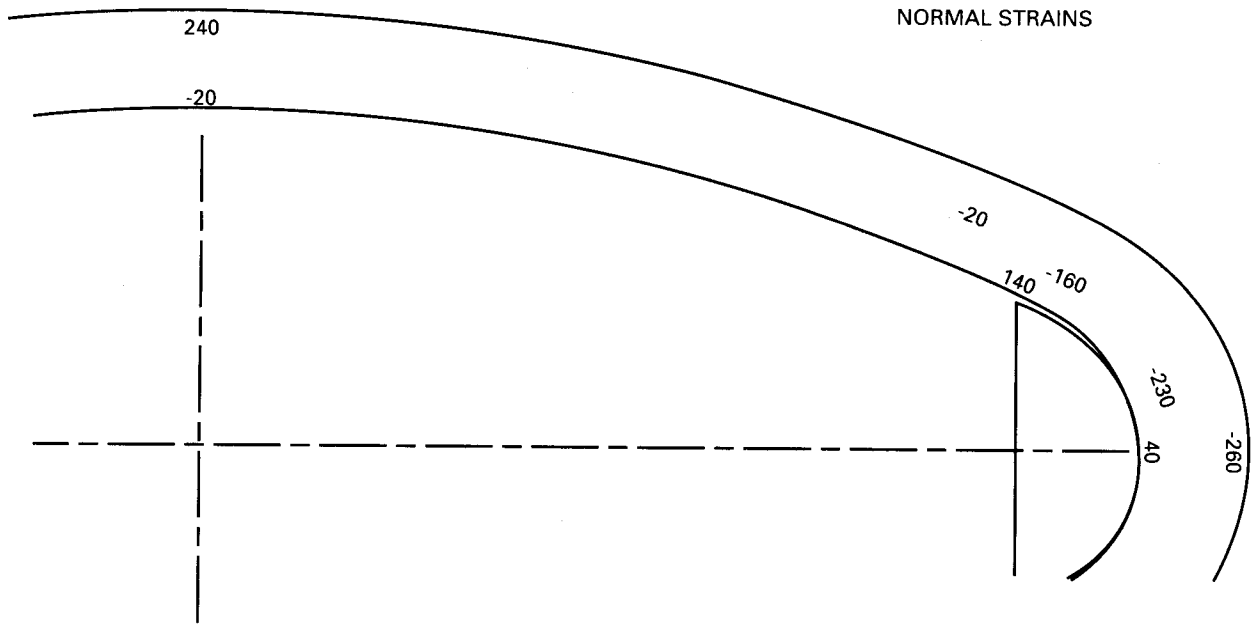


Figure 9b. Normal strains recorded after cutting.

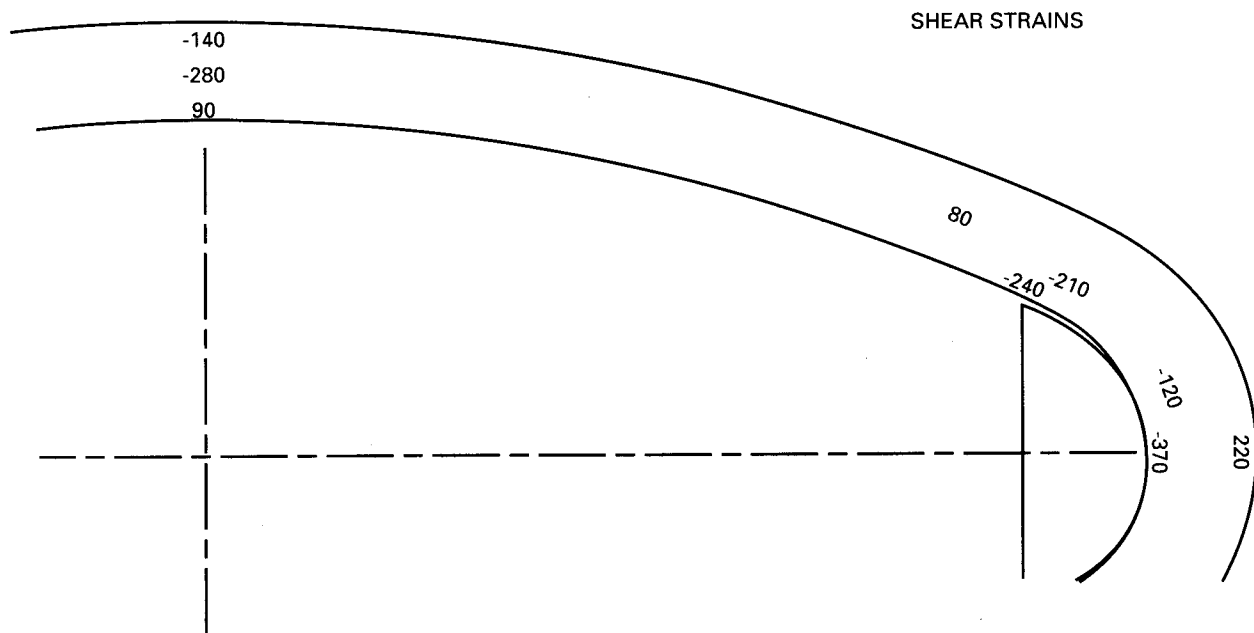


Figure 9c. Shear strains recorded after cutting.

Table 2. Final strain values after completing saw cuts.

Location	Orientation	Recorded Strain (microstrain)
MXAI	N	-20
	S+	90
	L	-890
MXAM	N	gage lost
	S-	-280
	L	200
MXAO	N	240
	S+	-140
	L	500
T2XAM	N	-20
	S-	80
	L	-10
TDXAI	N	140
	S+	-240
	L	-700
T1XA.33	N	-160
	S-	-210
	L	-200
C2XA.33	N	-230
	S-	-120
	L	-110
C1XAI	N	40
	S+	-370
	L	-870
C1XAO	N	-260
	S+	220
	L	640
M1IM	L	-950
TM1IM	L	-770

Table 3. Engineering constants of Brunswick shells.

Longitudinal (x 10 <sup>6</sup> psi)	Radial (x 10 <sup>6</sup> psi)	Transverse (x 10 <sup>6</sup> psi)	Interlaminar Shear (x 10 <sup>6</sup> psi)		In-plane Shear (x 10 <sup>6</sup> psi)	Poisson's Ratio		
			G <sub>21</sub>	G <sub>23</sub>		v <sub>21</sub>	v <sub>23</sub>	v <sub>13</sub>
E <sub>1</sub>	E <sub>2</sub>	E <sub>3</sub>	G <sub>21</sub>	G <sub>23</sub>	G <sub>13</sub>	v <sub>21</sub>	v <sub>23</sub>	v <sub>13</sub>
5.802	1.518	1.518	0.765	0.593	0.765	0.07	0.281	0.268

The expressions for the  $C_{ij}$  values in terms of the engineering constants are found elsewhere (for example, in reference 6).

Even in computing stresses only in the 1–2 plane, transverse strain (i.e.,  $\epsilon_3$ ) information is still required. Measuring transverse strains through the thickness is not trivial, and certainly not practical with conventional strain gages if they are not inserted during part fabrication. Transverse strains could have been measured on the inside and outside ring surfaces, but that option was neglected. It was felt that residual strains in the transverse direction were to be governed primarily by Poisson effects and would be of relatively small magnitude.

One assumption to consider for stress computation is that of a plane strain condition (i.e., to assume the transverse strains are essentially of zero magnitude). Another approach is to assume that strain magnitudes in the transverse direction are equal to those occurring in the normal (i.e., radial) direction. Since the material is transversely isotropic, this assumption would be valid if all the strains occurring in the plane of isotropy (i.e., the 1–3 plane) were governed by Poisson effects.

Table 4 compares stresses computed from these two approaches, the plane strain assumption versus the three-dimensional case where transverse strains are assumed to be equal to the radial strains. The difference in stresses between the two approaches is slight.

Table 4. Residual stresses.

Gage Location	Longitudinal $\sigma_1$ (psi)	Radial $\sigma_1$ (psi)	Int. Shear $\sigma_1$ (psi)	Longitudinal $\sigma_1$ (psi)	Radial $\sigma_1$ (psi)	Int. Shear $\sigma_1$ (psi)
MXA1	5458	561	69	5470	571	69
MXAM						
MXAO	-3202	-704	107	-3344	-826	107
T2XAM	73	40	-61	85	50	-61
TDXAI	4200	177	184	4118	105	184
T1XA.33	1319	390	161	1413	472	161
C2XA.33	809	456	92	945	573	92
C1XAI	5300	447	283	5276	427	283
C1XAO	-3762	63	-168	-3608	195	-168

The significance of these residual stresses is better understood when they are compared to in-service shell stresses. Table 5 lists the general location and magnitude of critical stresses typically experienced by the composite shell under hydrostatic pressure. These results, taken from reference 7, were gleaned from finite element results on one<sup>1</sup> particular Brunswick shell transducer configuration subjected to 350-psi hydrostatic pressure. Table 6 lists select gages located in the vicinity of the critical stress locations, and states whether or not the residual

<sup>1</sup> Reference 7 compares six Brunswick shells, each possessing relatively minor differences in thickness. Stresses from shell #3 in that study were selected because it was the only one that did not form a gap at the D-insert when subjected to 350 psi. A prime effect of gapping is to greatly increase the radial stress at the D-insert contact region.

stresses at those locations are additive or in opposition to the critical stresses. Table 6 also lists the magnitude of the residual stresses as a percentage of the critical stress values.

Table 5. Critical stresses experienced under hydrostatic pressure (reference 7).

	Longitudinal $\sigma_1$ (psi)	Radial $\sigma_2$ (psi)	Int. Shear $\sigma_5$ (psi)
Critical stress values and locations	42,886 psi at flat inner surface	1,691 psi at D-insert contact region	
	-57,796 psi at curve inner surface	-9,436 psi at D-insert contact region	-5,256 psi at transition neutral axis

Table 6. Residual stresses compared to critical stresses listed in table 5.

Gage Location	Longitudinal $\sigma_1$ (psi)	Radial $\sigma_2$ (psi)	Int. Shear $\sigma_5$ (psi)
MXAI	<i>Additive (13%)</i>		
T2XAM			<i>Additive (1%)</i>
TDXAI	<i>In opposition (-7%)</i>	<i>Additive (10%) or In opposition (-2%)*2</i>	
T1XA.33			<i>In opposition (-3%)</i>
C1XAI	<i>In opposition (-9%)</i>		

## CONCLUSIONS

The test data revealed that the inside fibers of the shell were under residual tension and the outside fibers were under residual compression, analogous to a bent beam. This corroborates the inward bending behavior that was observed after the first cut was made (figure 6).

When compared to critical stresses experienced by the shell in-service, residual stresses are both beneficial (being in opposition to those stresses) and adverse to these stresses, depending on the shell location at which they are evaluated. In either case, they tend to be a small percentage of critical in-service.

---

<sup>2</sup> Finite element results (references 4, 5, 6) indicate that large stress gradients can occur at the D-insert contact region. Residual peel stress recorded at location TDXAI may be either *additive* or *in opposition* to radial stresses at the location depending on the specific service pressure at which they are evaluated.

## REFERENCES

1. Sanders Surveillance Systems Division. Contractor's Monthly Progress and Status Report, "High Power Acoustic Projector, Report No. 13," Contract N66001-86-C-00227. June 1988.
2. Maltby, J. D. "Static Structural Tests on Composite Flextensional Transducer Shells," NOSC Technical Report 1447, October 1991.
3. Maltby, J. D. "Evaluation of Production-Grade Class IV Flextensional Transducer Shell," NRaD Technical Report 1604, April 1993.
4. Shaw, R. C. "Finite Element Analysis of Composite Flextensional Transducer Shell," NOSC Technical Report 1467, December 1991.
5. Shaw, R. C. "Structural Analysis of Flextensional Transducer—Progress Report No. 4," NRaD Memorandum Ser 933/04-92. 28 January 92.
6. Tsai, S. W. *Composites Design*, Think Composites, Dayton, Ohio. Third Edition, pp. 3-1 to 3-8. 1987.
7. Shaw, R. C. "Thickness Tolerance Study of Brunswick and Fibertek Shells," NRaD Memorandum Ser 933/74-92. 6 November 1992.